Marine Environmental Research 202 (2024) 106806

Contents lists available at ScienceDirect

Marine Environmental Research

journal homepage: www.elsevier.com/locate/marenvrev

Expanding sample volume for microscopical detection of nanoplastics

Arto Hiltunen [a,*], Joona Huopalainen [b], Ermei Mäkilä [c], Sirkku Häkkilä [d], Pia Damlin [b], Jari Hänninen [a]

[a] Archipelago Research Institute, Biodiversity Unit of the University of Turku, 20014, Finland
[b] Materials Chemistry Research Group, Department of Chemistry, University of Turku, 20014 Turku, Finland
[c] Department of Physics and Astronomy, University of Turku, 20014, Finland
[d] Laboratory of Aerobiology, Biodiversity Unit of the University of Turku, 20014, Finland

ARTICLE INFO

Keywords:
Nanoplastic
Chemical digestion
Seawater
Electron microscopy
Raman microscopy
SERS

ABSTRACT

The extent of nanoplastic pollution has raised severe environmental and health concerns. While the means for microplastic detection are abundant, improved tools for nanoplastic detection are called-for. State-of-the-art microscopic techniques can detect nanoplastics down to tens of nanometers, however, only from small sample sizes (typically ~ 10 μl). In this work, we describe a method that enables sampling of 1 l of seawater by the means of correlative Raman- and SEM-techniques. This is achieved by adapting common microplastic sample purification protocols to suit the nanoplastic study. In addition, we decorate a membrane filter with SERS-property to amplify the Raman signals. Together, the purification method combined with the use of the SERS-activated-membrane-filter enables identification and imaging of individual nanoplastic particles from significantly larger sample sizes than before. In the nanoscale the average recovery rate is 5 %. These results aim to provide useful tools for researchers in the fight against plastic pollution.

1. Introduction

It has been estimated that 60% of all plastics ever made, has been discarded either in the landfills or in the environment (Geyer et al., 2017). This has caused a global littering problem which was acknowledged in scientific literature already 50 years ago (Carpenter and Smith, Jr., 1972; Venrick et al., 1973). What makes the plastic waste problem especially challenging to manage is the breakage of the plastic materials into small pieces called micro- and nanoplastics, depending on how small they are. In this paper, we use the convention to call 5 mm–1 μm plastic particles as microplastics and 1–999 nm particles as nanoplastics. The breakage is thought to be caused by mechanical abrasion, UV-light, or digestion by small animals (Dawson et al., 2018; Ivleva et al., 2017; Gigault et al., 2016; Hernandez et al., 2023). Moreover, the most recent research shows that even brand new plastic products release large numbers of small plastic particles during usage (e.g. infant drinking bottles or tea bags) (Hernandez et al., 2019; Li et al., 2020). Hence, small plastic particles from whichever aforementioned origin, are now found on land, at sea, and in the air, even in the most remote places on Earth, down to sediments dated back to the 18th century (Brahney et al., 2020; Wahl et al., 2021; Bergmann et al., 2019; Materić et al., 2020; Dimante-Deimantovica et al., 2024).

While the harm from large plastic pieces to humans is mainly aesthetic (e.g. trashing of beaches) the micro- and nanoplastics have raised a health concern (Lim et al., 2021). Owing to their small size micro- and nanoplastics can enter the human body: Ragusa et al. reported microplastics in human placentas and Leslie et al. reported microplastics and nanoplastics in blood (Ragusa et al., 2021; Leslie et al., 2022). In general, it is thought that particles smaller than 1 μm may enter cells and particles smaller than 200 nm may cross the blood–brain barrier raising concern that the plastic might reach the brain (Lim et al., 2021).

The methods to study microplastics are well established, however the means to study nanoplastics are still incomplete. According to a recent review, nanoplastics are in most cases detected using pyrolysis coupled to gas chromatography-mass spectrometry (Py-GC-MS) (Mandemaker and Meirer, 2023). While the Py-GC-MS has proven to be extremely useful tool, and provided us with the first estimations on the nanoplastic concentration (μg/l) in various different environments, the shortfall of the method is that it cannot provide the particle count nor the size distribution in the sample. As, for example, the particle size determines how deep in the body they can travel, it is of utmost importance to have data on the particle counts down to the nanosize. Very recently, Bauten et al. reported a promising way to use flow cytometry to count nanoplastics using polymer binding peptides, but the application to environmental samples is yet to be demonstrated (Bauten et al., 2023).

* Corresponding author.
E-mail address: arto.hiltunen@utu.fi (A. Hiltunen).

https://doi.org/10.1016/j.marenvres.2024.106806
Received 22 March 2024; Received in revised form 19 September 2024; Accepted 16 October 2024
Available online 24 October 2024
0141-1136/© 2024 The Authors. Published by Elsevier Ltd. This is an open access article under the CC BY license (http://creativecommons.org/licenses/by/4.0/).

Raman microscopy has been shown to be an efficient technique to detect nanoplastics. Many groups have developed methods to find nanoplastics using Raman from within relatively clean sample matrices which do not require purification such as tap water or ultrapure water (e.g. Milli-Q) (Winkler et al., 2022; Schwaferts et al., 2020; Zhang et al., 2020; Sobhani et al., 2020; Yoo et al., 2022). In addition to Raman, microscopic images have been obtained from clean matrices using Scanning Electron Microscopy (SEM) combined with X-ray Photoelectron Spectroscopy (XPS) and Fourier-Transform Infrared Spectroscopy (FTIR) (Hernandez et al., 2019) or Scanning Transmission X-ray Microscopy (STXM) and Near Edge X-ray Absorption Fine Structure (NEXAFS) combined with Transmission Electron Microscopy (TEM) (Yang et al., 2021). In contrast to ultrapure water, environmental samples are more complicated to analyze (e.g. sea or lake water) due to vast amount of organic and inorganic matter present in the sample relative to the targeted plastics. Despite the challenging matrix, recent literature describes success in nanoplastic detection from natural waters using Raman techniques, namely, Raman tweezers,(Gillibert et al., 2019) and SERS (Surface Enhanced Raman Spectroscopy) (Chang et al., 2022; Lv et al., 2020; Hu et al., 2022a). However, the sample size so far has remained low, being typically 10 μl or "a drop" of unconcentrated and unpurified water. If the sample is not purified (i.e. not chemically digested) it will hamper the nanoplastic analysis, in particular, when using microscopic methods. Firstly, the small nanosized plastic particles might get buried under the organic matter making it impossible to image them. Secondly, identifying the plastics based on their Raman spectrum will be complicated as well due to background fluorescence signal from the organic matter. In fact, several authors have acknowledged the problem caused by the background signal when working with unpurified samples (Xu et al., 2020; Schmidt et al., 2021; Lv et al., 2020; Chang et al., 2022). Moreover, to utilize SERS effectively, the examined nanoplastics must be within a few nanometers of the metal surface (Stiles et al., 2008). Therefore the nanoplastic particle under investigation should ideally lie on the surface of the SERS-substrate without any matter in between.

The lack of a suitable purification protocol designed for microscopic investigation of complex sample matrices is essentially limiting the sample size to a drop. Concentrating a larger sample would also concentrate the organic and inorganic matter which would then bury the small nanoplastics making the use of microscopic methods impossible. To solve this problem, in this work, we show how to purify 1 l of seawater to such detail that individual nanoplastic particles can be identified using Raman spectroscopy and high magnification images obtained using scanning electron microscopy (FESEM). To assist in the detection of nanoplastics, a SERS-activated-membrane-filter is used to filter out the final reagent allowing direct observation of the particles from this very same filter. As far as we know, this is the first demonstration of reaching nanoscale resolution using microscopic techniques from such large sample size of actual seawater.

2. Results and discussion

In this section we first introduce the chemical digestion protocol designed for nanoplastic research, and show how each reagent acts on the seawater sample. Next, we introduce the developed SERS-activated-membrane-filter and show how it amplifies the signals from small nanoplastics. Finally, we introduce the whole protocol by showing how the chemical digestion is used together with the SERS-activated-membrane-filter to find nanoplastic particles mixed with seawater.

2.1. The chemical digestion protocol

Common chemical digestion protocols for microplastic extraction from complex matrices include the use of acids (HCl, H_2SO_4 or HNO_3) bases (KOH or NaOH) and oxidizers (H_2O_2 or Fenton reagent) with varying order, combination, concentration, processing times and temperatures (Pfeiffer and Fischer, 2020; Al-Azzawi et al., 2020; Gulizia et al., 2022). Typically, in the last stage prior to microscopic examination the reagent is filtered out, sample is rinsed with water to remove reagent traces, and then analyzed. Based on existing literature on microplastics we have put together a chemical digestion protocol suitable for nanoplastics. From the multiple possibilities we optimized for digestion efficacy taking into account chemical compatibility of the filters and the reagent.

The digestion protocol was first tested with seawater without added nanoplastics in it, and the effect of each reagent was examined microscopically. Polycarbonate filters were used throughout as only the reagents' effects on the seawater components was examined, and therefore no SERS was needed.

We began by filtering 1 l of seawater onto a 200 nm pore size polycarbonate filter. Due to rather large amount of organic matter in the Baltic sea the 200 nm filter pore size was selected to enable reasonable filtering time.

The first row in Fig. 1 shows the retentate after filtering 1 l of seawater without any purification. The filter surface is covered with bacteria, diatoms and phytoplankton. Trying to distinguish individual nanosized plastics from within this matter that is several times larger (e.g. the length of bacteria is around 1–2 μm) would be extremely challenging. In addition, the organic matter can be highly fluorescent which would disturb the Raman measurements. The images thus clearly show the need for an efficient purification protocol.

For the first digestion reagent we selected H_2O_2 and the result can be seen in the second row of Fig. 1. The H_2O_2 has effectively removed all of the organic matter. Earlier literature suggests that other oxidizers, namely sodium hypochlorite (NaClO), would be more efficient than H_2O_2. However, in our experiments with the selected digestion time, temperature, added amount and concentration, we did not see any residue of organic matter when using H_2O_2. Therefore, we concluded that for our purposes the H_2O_2 was efficient enough. After the H_2O_2 digestion, there appeared still to be a lot of inorganic matter left (e.g. diatoms) that could be further digested with other reagents. Diatoms' siliceous shells cannot be digested using H_2O_2 but can be dissolved using NaOH (Ehrlich et al., 2010).

The result of NaOH digestion can be seen in 3rd row of Fig. 1. The diatoms have been effectively removed and the filter surface has become again cleaner. It is worth noting that, polycarbonate has limited resistance against NaOH, however we found that the selected overnight reaction in 0.1 M NaOH effectively removed the diatoms without causing any damage to the filter that would be visible by eye or the electron microscope.

After NaOH, the sample matrix was digested using HCl in case there was calcareous ($CaCO_3$) items (e.g. minerals or mollusc shells) left in the sample. The end result of the process seems ideal for the nanoplastic detection using spectro-microscopic techniques: individual particles are against the clean surface of the filter without any fluorescent background present.

Milder purification conditions could be achieved using enzymatic digestion protocols which are performed in aqueous solutions in close to neutral pH (5–9) (Löder et al., 2017). Avoiding strong chemicals would also reduce the risk of damaging the plastics during the purification. However, we selected the chemicals and their strength such that they have been shown to have no or very little effect on the most common plastics according to literature (Pfeiffer and Fischer, 2020).

2.2. SERS-activated-membrane-filter

Typically when using Raman to detect nanoplastics, SERS is employed to get enough signal from the tiny particles. The SERS-effect can be created by depositing the sample on a nanostructured metal substrate or by the addition of nanoparticles onto the substrate or onto the sample. The signal enhancement is a result of laser excitation of the

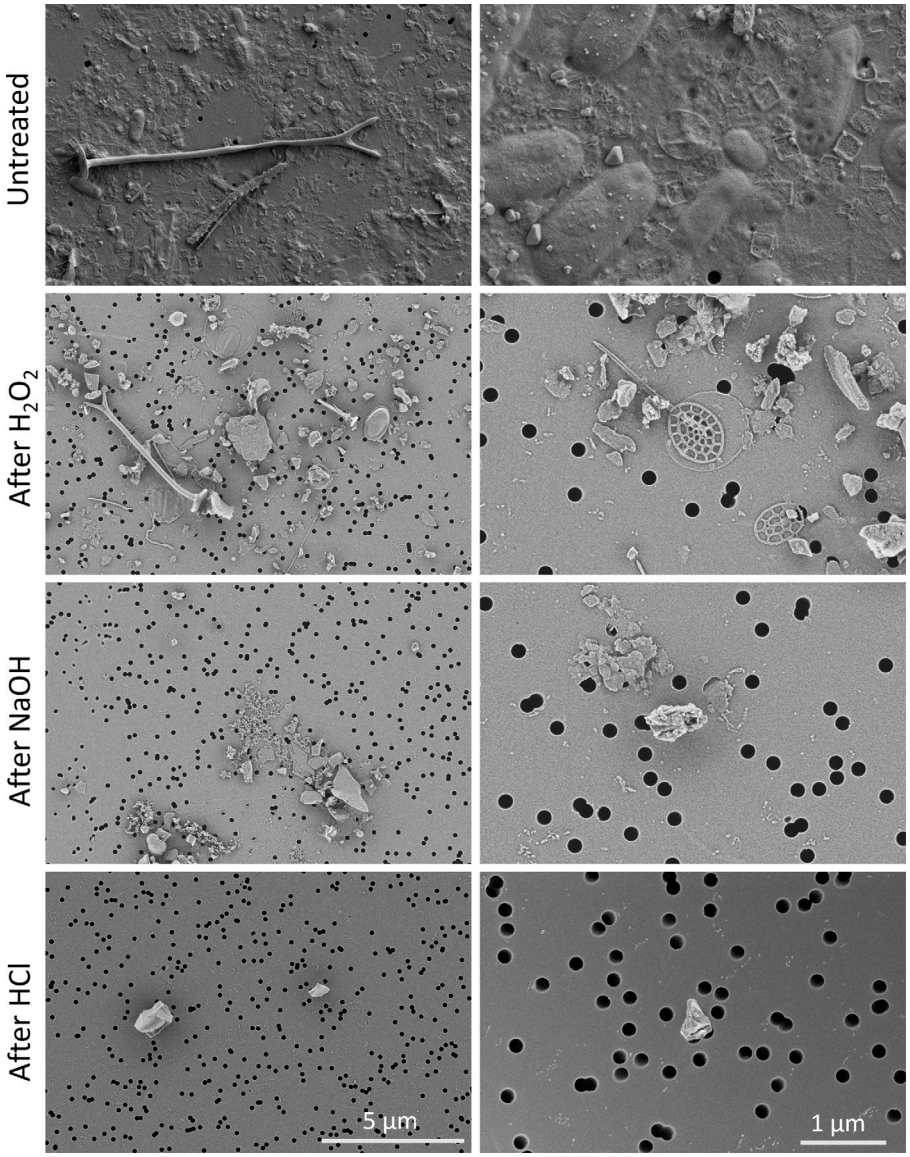

Fig. 1. The figure shows the sequential effect of each digestion reagent on the sample. The first row shows the filter surface after 1 l of seawater was filtered through it. In the last row the sample has been treated with H_2O_2, NaOH and HCl. Each column has the same magnification.

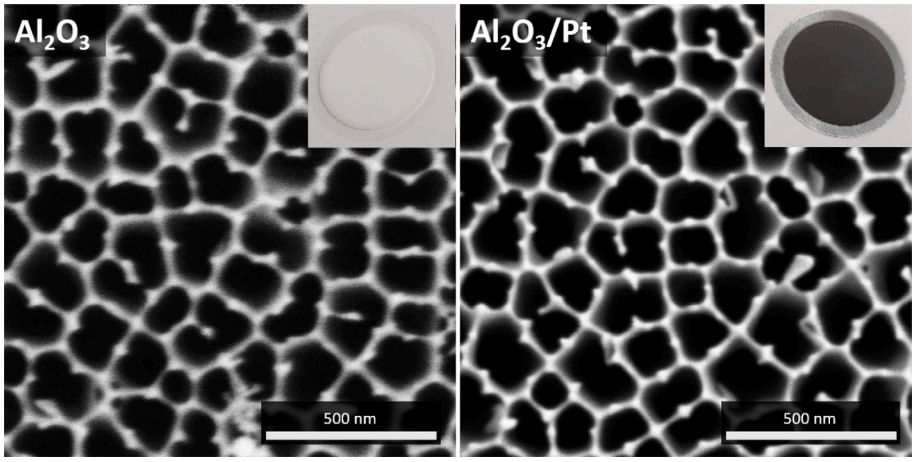

Fig. 2. The figure shows scanning electron microscope images of an uncoated Al_2O_3 filter surface (left) and the SERS-active platinum coated Al_2O_3 filter surface (right). The insets show photographs of the same filters.

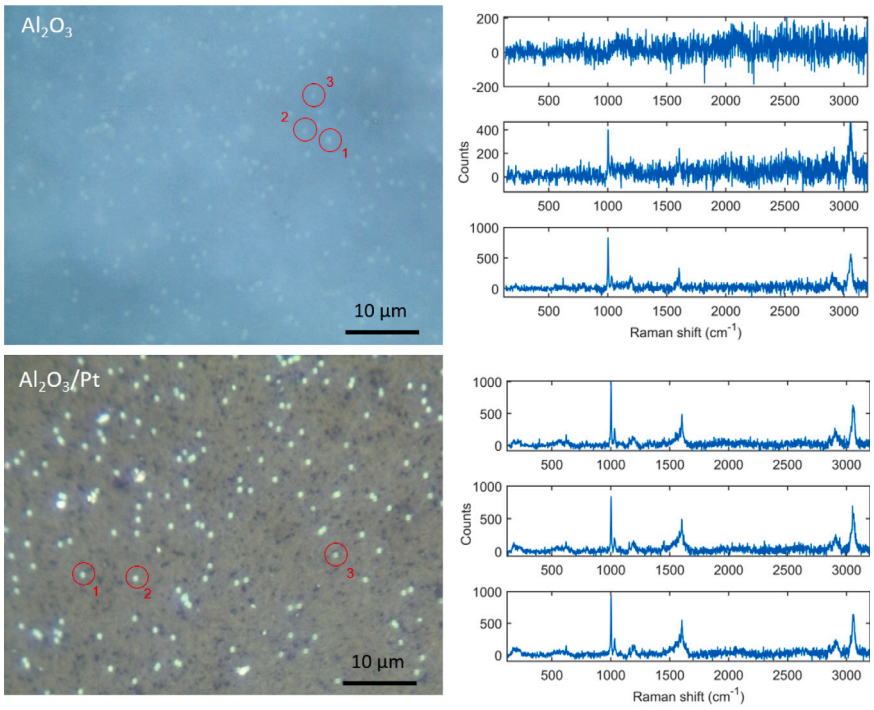

Fig. 3. The left column shows microscope images from the 500 nm polystyrene nanoparticles on the tested filter surfaces: uncoated Al_2O_3 (above), and platinum coated Al_2O_3 (below). Next to the microscope images are three Raman spectra recorded from the polystyrene nanoparticles on that filter surface. The spectra are arranged in order from 1 to 3, from top to bottom.

localized surface plasmon resonances (LSPR) which are located at the sharp features of the nanostructured surface (Sharma et al., 2012).

The SERS-function was generated onto alumina membrane filters (pore size 200 nm) via sputtering a thin layer of platinum onto the filters. Fig. 2 shows that the platinum coating creates an even conformal coating without any damage or alteration of the filter structure. The insets show that upon coating, the white Al_2O_3 gets a darker coloring. The functioning as SERS-substrates was tested with 500 nm polystyrene spheres. Fig. 3 shows a microscope image from both filter surfaces after a dispersion of polystyrene spheres was suction filtered through them. Next to the images, three representative Raman spectra measured from the spheres retained on the filter surface are provided. The coating produces two enhancements. Firstly, the plastic particles become more visible against a colored background owing to the contrast difference (white plastic against dark filter) compared to the uncoated Al_2O_3 filter where the white particles disappear in the white background. Secondly, a clear enhancement of Raman signal intensity is observed on the coated filters. Measurement from the Al_2O_3 filter (uncoated) results in noisy and weak signals while on occasion a decent spectrum is recorded. The Pt-coated filter gives a clear signal repeatedly.

The problem of not being able to detect the particles from the microscope image is known and efforts have been made to improve their visibility. In the context of nanoplastic research, Yang et al. (2022) reported that only particles larger than 500 nm could be optically resolved using their AgNW-based SERS-substrates, while Chang et al. (2022) reported that only particles larger than 800 nm were visually detected using their nanowell SERS-substrates. Even when using commercial Klarite substrate as background, it has been reported that plastic particles below 1 µm are challenging to distinguish directly from the microscopic image (Xu et al., 2020). In all these studies, rough surfaces were used as SERS-substrates, which can complicate the recognition of small particles. However, even against smooth surfaces, small plastic particles can be difficult to detect, if there is not enough contrast difference between the particles and the background. Oßmann et al. (2017) reported that colorless 1 µm PS particles were difficult to detect against white PC membrane both under white light and dark-field illumination. In their work, the PS particles turned clearly visible only under dark-field illumination after they were deposited on to black or metal coated PC-membrane. Here, owing to the improved contrast between the Pt-coated background, 500 nm PS spheres are easily detected from the Pt-coated filter surface under standard reflected white light illumination. As a result, the Raman spectra of individual nanoplastics can be acquired using point measurements thus no highly time-consuming Raman mapping is needed.

2.3. Demonstration with seawater-nanoplastic mixture

Next, the developed chemical digestion was used together with the SERS-activated-membrane-filter. The whole protocol is schematically shown in Fig. 4. In brief, the seawater is filtered through a 200 nm pore size PC filter which is then digested in H_2O_2, NaOH, and HCl. The H_2O_2 and NaOH are filtered out using PC filters but the SERS-active Al_2O_3/Pt-filter is used to filter out the HCl, thus allowing for the imaging of nanoplastics directly from this filter.

The method was tested with a mixture of seawater and nanoplastics fabricated in the laboratory from consumer products according to El Hadri et al. (2020). We chose to test the method with environmentally relevant concentrations at 53±8 µg/l. This concentration falls within the reported range of nanoplastics concentrations in the environment, which can vary from 4.5 µg/l to 563 µg/l (Materić et al., 2022a,b). Fig. 5 shows the Al_2O_3/Pt-filter surface after the plastic-seawater mixture has gone through the digestion protocol. Individual particles can be seen on the filter surface and be tested whether they are plastic or not using Raman spectroscopy. Our digestion protocol has limitations, which will be discussed in more detail later. Consequently, other particles, such as sand, are also present on the filter surface. However, two smallest objects in this frame (Fig. 5) that were identified as plastics based on their Raman spectrum (given in Fig. 6) has been marked into the image. The spectra from the nanoplastics are in good accordance with spectrum measured from the original material from which the nanoplastics were

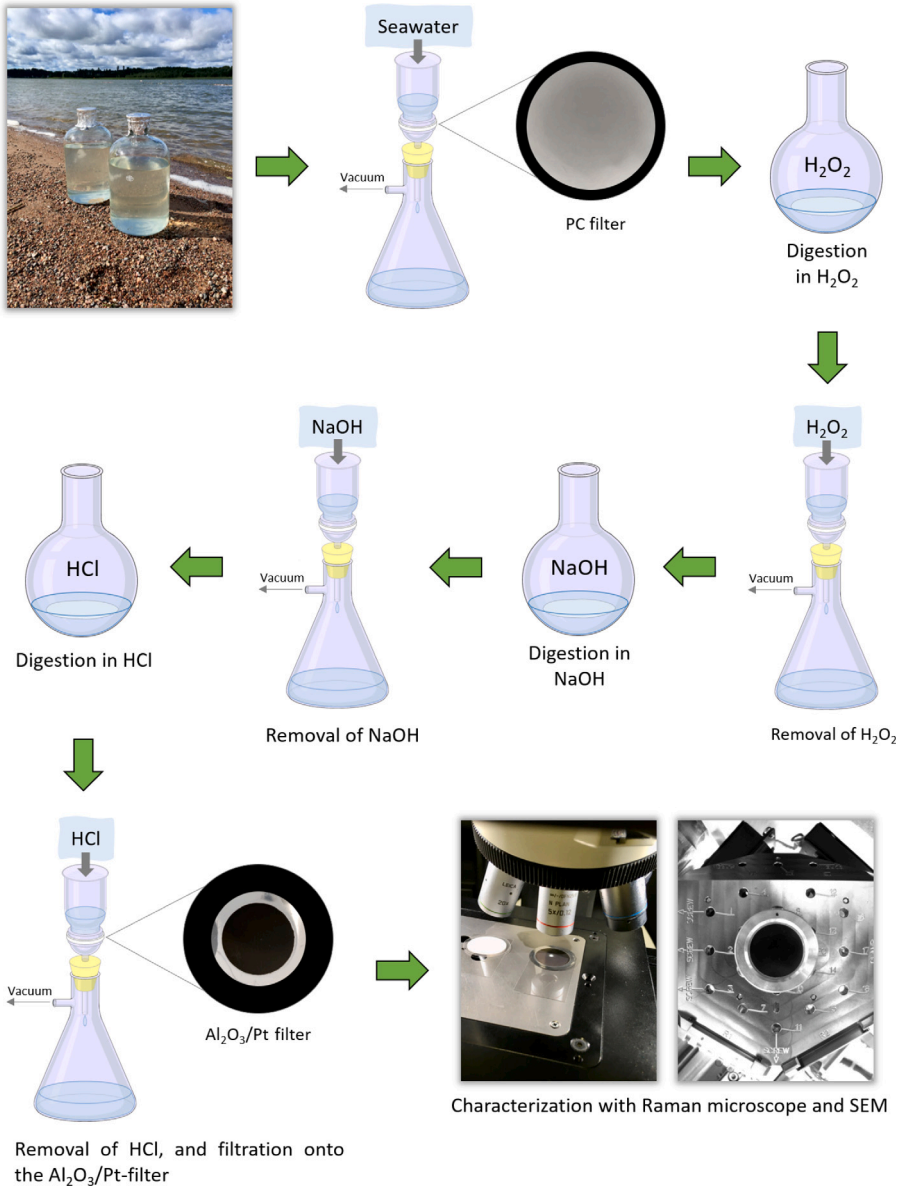

Fig. 4. A scheme depicting the developed process for identifying and obtaining high magnification images from nanoplastics contained in seawater.

prepared. It appears that the purification protocol does not damage or alter the chemical fingerprint of the nanoplastics. Moreover we have not observed any alteration in the morphology of the nanoplastics after the processing compared to before processing (SEM images provided in Supporting Information Figure S4). Owing to sufficient purification, the objects could be identified using fast point measurements from individual particles rather than time consuming Raman mapping. For correlative Raman-electron microscope imaging, the coordinates of the particles on the filter are marked (at the Raman instrument), and then located again with the SEM. The size of the two smallest identified plastics in the presented frame were 1092 nm × 780 nm and 936 nm × 640 nm for particles 1 and 2, respectively (the measured distances are marked in Supporting Information Figure S5).

While we can identify individual particles, we also notice the presence of particle clusters or aggregates. Obviously, the clusters complicate Raman spectrum acquisition as we operate at the limit of the optical resolution of the Raman microscope. SEM combined with EDS was used to provide further verification of particle composition. According to the EDS maps, particle 1 in Fig. 7 is confirmed to be carbon, which, along with the Raman spectra provided in Supporting Information Figure S6, indicates that it is plastic. The size of it is 786 nm × 462 nm. In fact, it appears that the plastic particle itself is a cluster of four or more smaller plastic particles. Particles 2 and 3 are made of silicon and oxygen suggesting they are sand (SiO_2). The particles other than plastic still present in the sample after purification are discussed in detail later in the text. Recently, Mattsson et al. (2024) used platinum coated PC-membranes to filter large amounts of water, and demonstrate trapping of a microplastic particle (~ 500 μm) using correlative SEM-Raman technique.

Many of the current nanoplastic extraction protocols presented in the literature rely on minimal sample preparation prior analysis limiting the sample size to a drop due to disturbances caused by the organic and inorganic matter in the sample. The Raman tweezers (Gillibert et al., 2019) technique can detect nanoplastic particles from 10 μl of seawater cast between two microscope slides, however, no electron microscope images can be correlated with the detected particles due to the encapsulation.

In fact, only a few works that demonstrate SEM imaging of nanoplastics from within environmental samples exist. Aggregating several nanoplastic particles into a cluster together with silver nanoparticles to

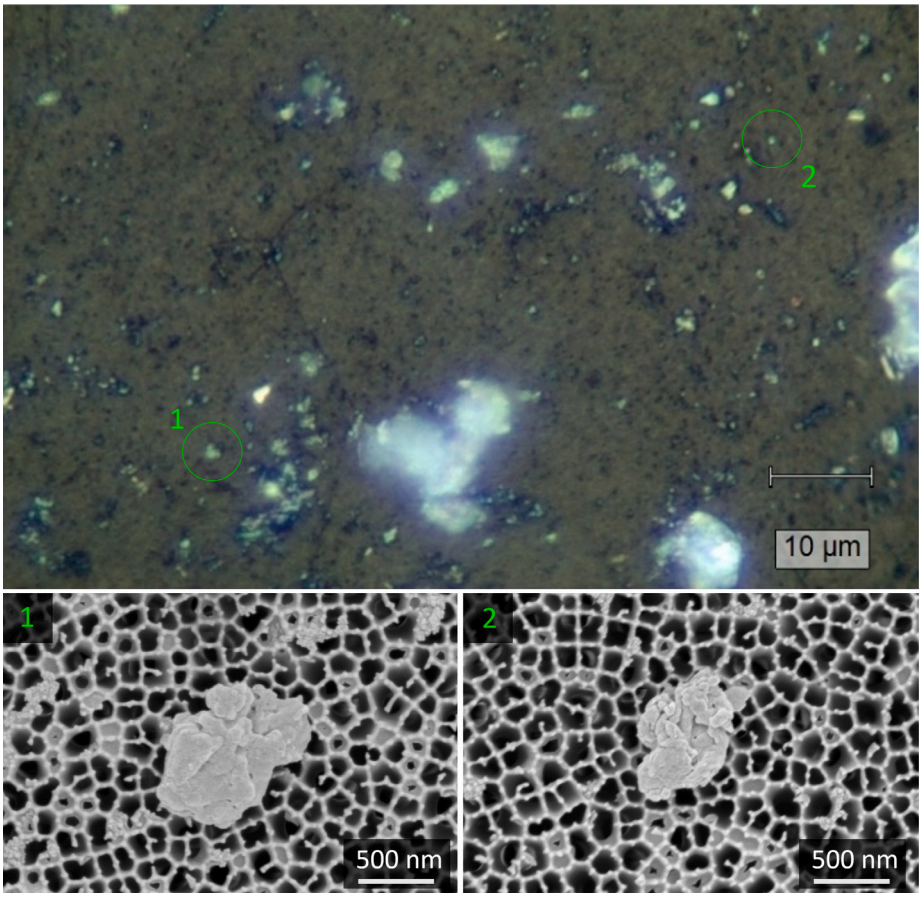

Fig. 5. The optical microscope image (connected to Raman) above shows the plastics collected onto the Al_2O_3/Pt-filter surface after the sample was treated according to the developed protocol. The electron microscope images below show the smallest particles that were identified as polystyrene according to their Raman spectrum.

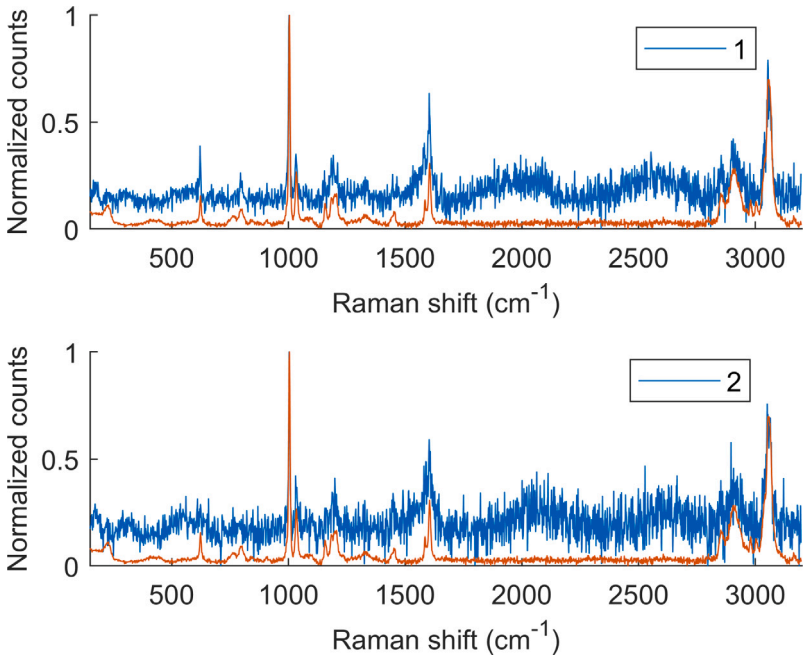

Fig. 6. The figure shows Raman spectra (with blue) from particles 1 and 2 that were presented in Fig. 5. The spectra are compared to a spectrum (with orange) that was recorded from the original large piece of plastic from which the nanoplastics were made.

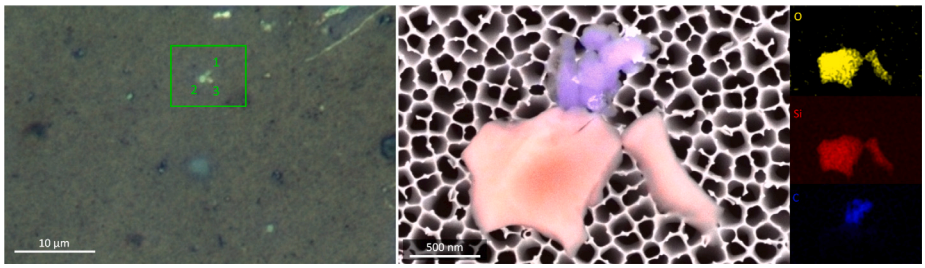

Fig. 7. A cluster of three particles imaged with optical microscope (left), and with both overlaid and individual element maps (right).

create the SERS-effect has been suggested. Electron microscope images from the clusters were successfully provided (Hu et al., 2022b; Lv et al., 2020). Chang et al. (2022) were able to find single particles rather than clusters using Raman mapping and subsequently imaging them with SEM. However, their sample size was, as well, limited to 10 µl and the difficulty of analyzing an environmental sample was acknowledged. Moon et al. (2024) used shrinking surface bubble deposition (SSBD) technique to detect nanoplastics in ocean water using the combination of SEM and Raman spectroscopy. While they have taken a major step towards more accurate nanoplastic analyses, their sample size (200 µl) still remains small. Xu et al. (2020) were able to detect nanoplastic particles from air samples which they had digested in H_2O_2. They could image individual particles using correlative Raman and electron microscopy. However, as we have demonstrated, seawater is more complicated matrix than air and thus requires further purification and filtration steps. Therefore, as far as we know, we propose the first method to detect nanoplastic particles microscopically from seawater from a substantially larger sample size (1 l) than previously demonstrated (10–200 µl).

The main shortcomings of the method, as already pointed out, include occasional identification of particles other than plastic and the formation of aggregates, small or large. Fig. 8 shows element maps of two aggregates present in the sample obtained using the EDS (the spectra measured at locations 1–4 are given in the Supporting Information Figure S7). Carbon in the maps is marked with blue and thus is the polystyrene. The spectrum collected at location (3) indicates the presence of mainly C. The composition of the particles similar to locations 1 and 2 appears to be silicon oxides with Na and Mg, corresponding to beach sand and clay from the sample collection site. Some Pt-coated spherical aluminium oxide particles were also observed, as indicated by the spectrum obtained from location (4), suggesting their presence on the filter disc before the Pt coating. Fig. 8B shows another type of contaminant with same composition as at location 4, which are the small granular clusters colored with green (Pt) in the map. They as well are present on the filter surface fresh from the pack (for images see Supporting Information Figure S8). In SERS activation, the clusters are coated with Pt, and apparently breaking off from the filter disc and aggregating with the plastic and sand particles during the filtration process.

In the herein described purification method the water samples were let to settle (in dark and at 3 °C) during which time most of the sand precipitated on the bottom of the flask. It appears that this was not sufficient to remove all the sand. We know from microplastic literature that density separation using heavy liquids can be used to remove sand and other sediment material from samples (Saarni et al., 2021). Because of the colloidal nature of nanoplastics, density separation methods are more challenging to apply, but possible if centrifugation is used (Minelli et al., 2018). Another way to remedy the issue would be to collect samples from deeper waters further away from the shore where there is less sand mixed with the water. Thus addition of heavy liquid separation or any other additional purification steps should be considered depending on the water type at the sample collection site.

Despite the limitations, as we have demonstrated, nanoplastic particles can be detected to a reasonable degree from seawater samples. To quantify the efficacy of our process we measured its particle recovery rate i.e. how many percent of added test particles can be recovered after the processing. To establish a universally applicable reference that is both replicable and enables reliable comparisons with other methods, we determined the recovery rate of the process using ultrapure water (Milli-Q) instead of environmental water. Environmental water sources will exhibit variations based on factors such as type (seawater, lake, river, etc.), time of the year, and location. Recovery rates in environmental water are expected to fall below that of what is measured in ultrapure water due to more complicated medium.

To calculate the recovery rate, minimum and maximum dimension of a plastic particle was measured (see Supporting Information Figure S2 for an example image), and the recovery rate is thus reported as a function of both dimensions. The results are presented in Fig. 9. The average efficiency for particles having maximum dimension between 200–1000 nm is 5.5%. No smaller than 200 nm particles are recovered as the filter pore size was 200 nm. The average recovery rate for particles having their minimum dimension between 100–1000 nm is 8.6%. A clear general trend is observed, where larger particles are recovered more efficiently than smaller ones.

Recovery rates for nanoplastics analyzed using *mass-spectrometry* based method range from 12.7 up to 100% (Cai et al., 2021). Surprisingly, we found no previous literature for comparing our recovery rates calculated from microscope images. That said, Hu et al. (2022b) reported a recovery rate of 87.5%–110%, contrasting significantly with our results. Unfortunately, they did not provide a description of how the values were measured, making a proper evaluation between the methods difficult.

While we targeted nanoplastics in this study, the microplastic collection efficiency was determined as well. Again, similar trend as for nanoplastics was observed. The average recovery rate for plastics being at most 1–10 µm in dimension was 36.6%, and when calculated according to the minimum dimension we got 47.8%. Tabulated values for recovery rates plotted in Fig. 9 are given in Supporting Information Table S1 and S2. In comparison with prior studies, Du et al. (2024) reported a 7% recovery rate for small microplastics in the 1–20 µm range. Our study clearly exceeds this reported rate. In fact, it appears that our recovery rate at around 10 µm approaches that what is typically reported for microplastics (< 5 mm) in water, which according to a recent review is on average 82% for low density polymers such as PS (Way et al., 2022).

Strategies to improve the collection efficiency could include the addition of common separation strategies in the process such as centrifugation or prefiltering in order to remove excess material from the water and more effectively collect plastics.

Background contamination of our laboratory and the contamination arising from the process itself was monitored during the test period. Level of contamination was measured by calculating particles from a control sample which was 1 l of ultrapure water (Milli-Q) processed with the method described in this paper. The most notable type of contamination is polycarbonate particles which we expect to arise from

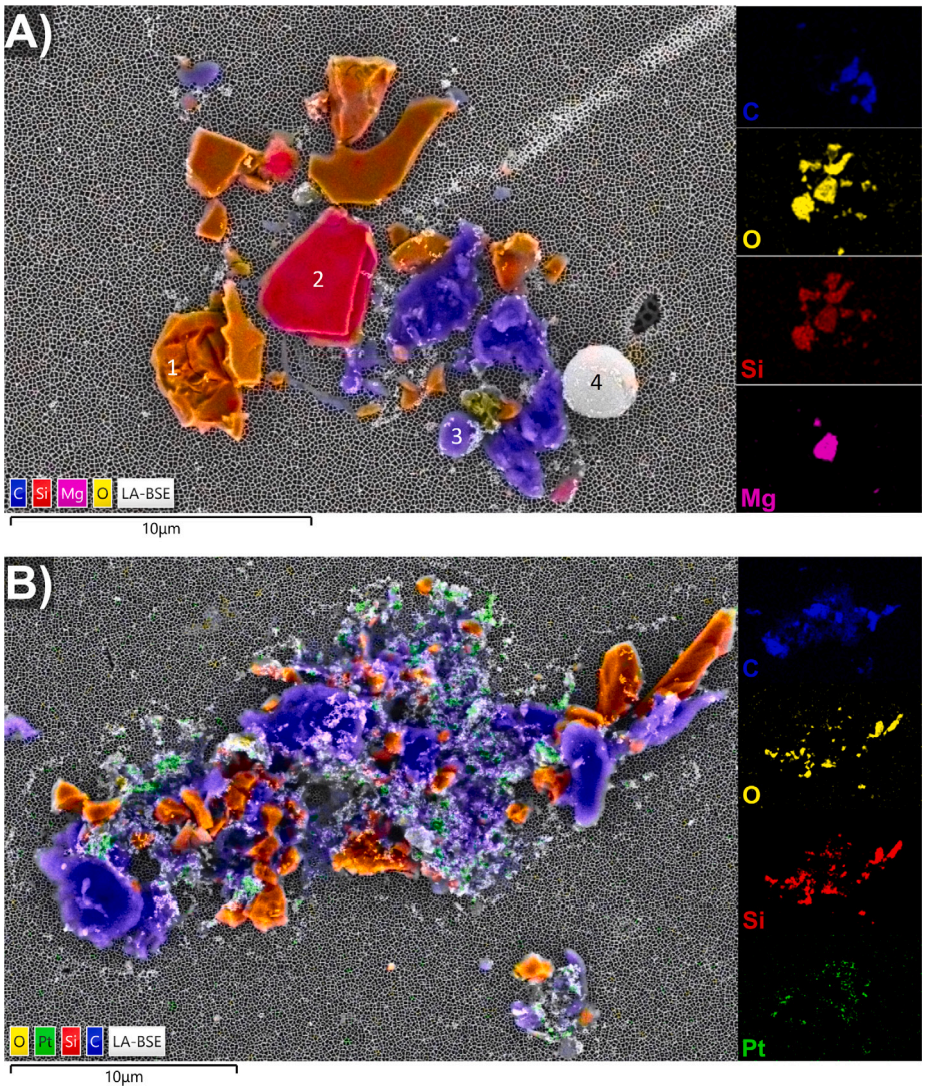

Fig. 8. Two examples of clusters detected in the sample after purification. Plastics are marked with blue (carbon), sand and clay are marked with orange (Si, O, Na) and red (Si, O, Mg). Platinum is marked with green.

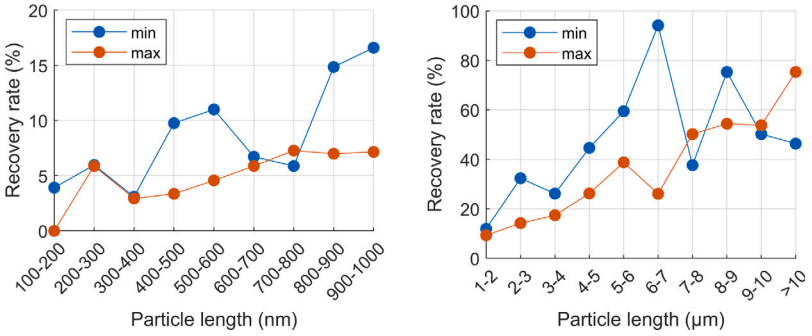

Fig. 9. Recovery rates for nanoplastics (left) and microplastics (right). Two graphs are shown per figure: one as a function of particle's largest dimension (max), and the other as a function of its smallest dimension (min).

the polycarbonate filters that were used. The PC contamination was 123 particles/1 mm^2, which is 10 times smaller than the recovered PS concentration (1082/mm^2). Moreover, PC does not belong in the most common plastics, thus its presence does not hamper the environmental analyses that target the PP, PET, PE. Other plastics in the laboratory equipment used in the process were teflon (filter grid holder and the support grid for the filters) and PP (support ring around Al_2O_3 filters), however teflon and PP were not detected in control samples.

Contamination not relating to the process but expected to be our laboratory specific were cellulose (Alves et al., 2016) (most likely from paper wipes), graphite (Ferrari, 2007) and the blue pigment copper phthalocyanine (Zou et al., 2020) based on their Raman spectra (given

in Supporting Information Figure S9). As they are not plastics, their presence does not hamper the plastic analyses. Each laboratory is expected to have their own specific background contamination, and obviously efforts should be made to minimize it. Fortunately, as long as the contamination does not involve plastic, it does not significantly impede the analyses, except for the additional time required to measure extra particles.

3. Materials and methods

3.1. Sampling and storing of seawater

Seawater samples were collected from the Baltic Sea at Ispoinen Beach (60°24'52"N 22°15'33"E) on 3.10.2022 and Kansanpuisto Beach (60°25'35"N 22°10'59"E) on 14.2.2023 both locating in the coast of Turku, Finland. Sampling was done by filling 5 l glass bottles with surface water at the sampling sites. Filled bottles were closed with ground joint glass stopper and covered with a piece of aluminium foil to protect the sample from contamination as shown in the photograph in Fig. 4. The samples were stored at 3 °C in dark until further processing. During the storing, matter denser than water (e.g. sand) sank to bottom of the sampling bottle.

3.2. Chemicals for sample matrix digestion

Hydrogen peroxide (H_2O_2, 30% analytical reagent grade) was supplied from Fischer Scientific. Hydrochloric acid (HCl, 37%, analytical reagent grade) and sodium hydroxide (NaOH, pellets, 98.9%) were supplied from VWR. NaOH pellets were dissolved in Milli-Q water to achieve 0.1 M NaOH solution. HCl was diluted with Milli-Q water to achieve 10% HCl solution. All these chemicals were filtered through polyethersulfone (PES) membrane filter (Sartorius Type 15407, 0.2 μm pore size, 47 mm diameter) prior use.

3.3. The chemical digestion protocol

1 l of seawater (Ispoinen Beach) from the 5 l sampling bottle was carefully poured into a large flask trying to leave the sand behind. Next, the seawater was poured onto a 200 nm pore size polycarbonate (PC) filter, and suction filtered. Residue left on the filter was collected by transferring the filter into round-bottom flask. The leftover filtrate was discarded. For the first digestion step, 30 ml of 30% H_2O_2 was added into the flask. A recovery bend was added to the flask to serve as a cap to minimize the risk of contamination but simultaneously allowing gases to evaporate freely (also applied in the further steps). The filter was bathed in the H_2O_2 for a week. During this time, the flask was at 50 °C water bath for 3 consecutive days 6 h/day (on 2nd, 3rd and 4th day). In the morning of each day of heating, 10 ml of 30% H_2O_2 was added into the flask. Rest of the time the flask was kept at room temperature.

After the week, the sample in H_2O_2 was poured onto a new PC filter and suction filtered. The flask (where the first filter still remains) was rinsed with 30 ml of Milli-Q water for 6 times to collect all particles. The rinsing water was poured onto the new PC filter and suction filtered. Next the new filter was moved into clean round-bottom flask where 30 ml of 0.1 M NaOH was added. The sample was digested in NaOH for 24 h at room temperature.

After the 24 h, the sample in NaOH was poured onto a new PC filter, and suction filtered. The flask was rinsed with 30 ml of Milli-Q water for 6 times. After the sample in NaOH and the rinsing Milli-Q water were suction filtered, the filter was moved into a round-bottom flask. 10 ml of 10% HCl was added and let the digestion proceed for 1 h at room temperature. Finally, the HCl was removed by filtering the sample through a new PC filter.

A small piece (< 1 cm^2) of PC filter was cut every time before the filter was moved into the round-bottom flask, in order to image the processing steps (presented in Fig. 1). These small pieces were taped onto pin mount specimen holders with carbon tape and sputtered with 10 nm of platinum prior SEM imaging.

3.4. SERS-activated-membrane-filter

Platinum (deposition thickness 12 nm) was sputtered onto Al_2O_3 membrane filters (Cytiva Whatman Anodisc Circle with Support Ring, 25 mm, 0.2 μm pore size) using Quorum 150 V ES+ sputter coater.

Spherical PS nanoparticles (Latex Microsphere Suspension, 10% w/w, mean diameter 0.50 μm, Catalog Number 5050 A) were purchased from Thermo Fisher Scientific. They were diluted 1000 times prior using (10 μl PS suspension to 10 ml Milli-Q water). Then 10 μl of the 1000x diluted PS suspension was pipetted into 30 ml of Milli-Q water, which was then filtered onto the Pt-coated (i.e. SERS-activated) or uncoated Al_2O_3 filters. After the filters had dried, they were characterized with Raman microscope.

3.5. In-house made polystyrene (PS) nanoparticles

The in-house made PS nanoparticle solution, was prepared as follows. Polystyrene packages from alimentary products were collected and washed with soap and water. Small amount of PS powder was prepared by sawing the packages with a hand saw. Next the powder was ground to nanosize using a ball mill the following way. Total of 1 g of white PS sawdust was added into 5 separate borosilicate glass vials (200 mg/each). 2 g of zirconium grinding beads (diameter: 1 mm) and 2 ml of ethanol were added into each vial. Vials were put into designated vial holder which was then attached into the planetary ball mill (Fritsch Pulverisette 7). Grinding duration and speed were chosen according to the study of El Hadri et al. (2020) (speed: 450 rpm, duration: 40 cycles of 3 min of grinding and 6 min of pause). After the grinding, the top 1 ml of each vial was collected into a new vial (a photograph shown in Supporting Information Figure S1). PS concentration of the resulted solution was calculated by filtering 1 ml of the solution through a filter (pore size: 200 nm) and weighing the retentate resulting in 0.53 ± 0.08 mg/ml.

3.6. Demonstration with seawater-nanoplastic mixture

1 l of seawater (Kansanpuisto Beach) from the 5 l sampling bottle was carefully poured into a large flask to leave the sand behind. Next, 100 μl of in-house made PS nanoparticle solution was added into the same flask and mixed. The resulting plastic concentration became 53 ± 8 μg/l.

The water was treated as described above in section *The chemical digestion protocol* with the exception that the HCl was removed by filtering the sample through the Pt-coated Al_2O_3 filter (instead of a PC filter), which was designed to act as the SERS-substrate. Prior characterization with Raman microscope and SEM, the filter was let to dry at room temperature.

After the filter had dried, small scratch was done in the middle of the filter with injection needle to mark the (0,0)-coordinate point according to which the plastic particles were located.

All steps until here were performed in Class II-level biosafety cabinets to protect the samples from contamination.

Then the filter was characterized with Raman microscope, and the smallest plastics were targeted. Raman spectra of found nanoplastics were compared to a spectrum, which was obtained from the same white PS plastic, from which the nanoplastics were made. Once a nanoplastic particle was found, its coordinates were noted down. Later, using the coordinates, the same PS nanoparticles were accurately found and high magnification images obtained with SEM.

3.7. Recovery rates calculation

The recovery rate was calculated by dividing the number of particles found in the sample filter by the number found in the reference filter and then multiplying the result by 100%. In more detail, the maximum and minimum dimension from all the plastic particles in an area was measured (see Supporting Information Figure S2 for an example measurement). Based on the measurements, the number of particles was classified according to their sizes (100–200 nm, 200–300 nm, …, 900–1000 nm, 1–2 μm, 2–3 μm, …, 8–9 μm, > 10 μm). Then the recovery rate was calculated according to formula:

$$\text{Recovery rate}_i = \frac{\text{count}_i^{sample}/\text{area}^{sample}}{\text{count}_i^{ref}/\text{area}^{ref}} \cdot 100\%, \quad (1)$$

where i = 100–200 nm, …, 900–1000 nm, 1–2 μm, …, 8–9 μm, > 10 μm, $count_i$ is the number of particles found corresponding to size range i, $area$ is the area from which the particles where counted, $sample$ refers to the sample under study, and ref refers to the reference sample where plastics are detected without losses.

The recovery rates presented in Fig. 9 were calculated from a sample where 100 μl of nanoparticle solution was mixed with 1 l of ultrapure water (Milli-Q) resulting in concentration of 53 ± 8 μg/l. The sample was processed as described above. As a reference sample the same amount of nanoparticle solution (100 μl) was directly pipetted onto the filter (Al_2O_3/Pt).

To calculate the recovery rates of particles up to 4 μm in size, 127 particles were found and measured on the sample filter from an area of 117 300 μm^2, while 427 particles were found in the examined area on the reference filter, which had an area of 27 600 μm^2.

Particles larger than 4 μm were counted from larger areas: 291 575 μm^2 and 219 528 μm^2 for sample and reference filter, respectively. The SEM image used in calculation (patched together from multiple smaller images) is presented in Supporting Information Figure S3. During the examination, 113 particles larger than 4 μm were found on the sample filter, while 191 particles were found in the examined area on the reference filter

3.8. Raman microscopy

The Raman instrument was Renishaw Qontor inVia Raman microscope equipped with Leica Microscope, a CCD detector and 1800 l/mm grating. Raman spectra were recorded at room temperature using 532 nm laser (RL532C50, Renishaw). The power of the laser was adjusted as high as possible without burning the PS spheres on the platinum coated filter (0.171 mW). The spectra were recorded on single scan using 100 s acquisition time and 100x objective. Peaks caused by cosmic rays were removed from the data, and baseline correction was applied using the inVia. The spectra are shown without any smoothing.

3.9. Electron microscopy (FESEM/EDS)

Electron micrographs and elemental analysis of the samples were taken with Apreo S (Thermo Scientific, The Netherlands) field-emission SEM, equipped with Ultim Max 100 energy dispersive spectrometer (EDS; Oxford Instruments, UK). High magnification images were collected using an acceleration voltage of 2 kV. For confirming the composition of the samples, elemental maps and EDS spectra were acquired using an acceleration voltages of 4–6 kV. Compositional analysis was done using AZtec 6.1. software (Oxford Instruments).

4. Conclusions

In this work we presented a method which would allow the identification and production of high magnification images of nanoplastics from 1 l of seawater using Raman and electron microscopy. We conclude that we have succeeded to increase the sample size from the common sample of some microliters up to one liter of actual seawater. How much water is enough to make a reliable nanoplastic analysis is yet to be determined. However, these results should open up new possibilities for researchers, and pave the way towards accurate analytical protocol for nanoplastic detection.

CRediT authorship contribution statement

Arto Hiltunen: Writing – original draft, Methodology, Investigation, Funding acquisition, Conceptualization. **Joona Huopalainen:** Writing – review & editing, Investigation. **Ermei Mäkilä:** Writing – review & editing, Investigation. **Sirkku Häkkilä:** Resources. **Pia Damlin:** Writing – review & editing, Supervision, Resources. **Jari Hänninen:** Writing – review & editing, Supervision, Project administration, Funding acquisition.

Declaration of competing interest

The authors declare the following financial interests/personal relationships which may be considered as potential competing interests: Arto Hiltunen reports financial support was provided by Weisell-foundation. If there are other authors, they declare that they have no known competing financial interests or personal relationships that could have appeared to influence the work reported in this paper.

Acknowledgments

We thank the Weisell Foundation and the Sakari Alhopuro Foundation for funding. The study has utilized research infrastructure facilities provided by FINMARI (the Finnish Marine Research Infrastructure consortium). The study contributes to the thematic collaboration of The Sea and Maritime Studies according to the strategy of Turku University.

Appendix A. Supplementary data

Supplementary material related to this article can be found online at https://doi.org/10.1016/j.marenvres.2024.106806.

Data availability

Data will be made available on request.

References

Al-Azzawi, Mohammed SM, Kefer, Simone, Weißer, Jana, Reichel, Julia, Schwaller, Christoph, Glas, Karl, Knoop, Oliver, Drewes, Jörg E, 2020. Validation of sample preparation methods for microplastic analysis in wastewater matrices—reproducibility and standardization. Water 12 (9), 2445.

Alves, Ana Paula P, de Oliveira, Luana PZ, Castro, Aloísio AN, Neumann, Reiner, de Oliveira, Luiz FC, Edwards, Howell GM, Sant'Ana, Antonio C, 2016. The structure of different cellulosic fibres characterized by Raman spectroscopy. Vib. Spectrosc. 86, 324–330.

Bauten, Wiwik, Nöth, Maximilian, Kurkina, Tetiana, Contreras, Francisca, Ji, Yu, Desmet, Cloé, Serra, Miguel-Ángel, Gilliland, Douglas, Schwaneberg, Ulrich, 2023. Plastibodies for multiplexed detection and sorting of microplastic particles in high-throughput. Sci. Total Environ. 860, 160450.

Bergmann, Melanie, Mützel, Sophia, Primpke, Sebastian, Tekman, Mine B, Trachsel, Jürg, Gerdts, Gunnar, 2019. White and wonderful? Microplastics prevail in snow from the Alps to the Arctic. Sci. Adv. 5 (8), eaax1157.

Brahney, Janice, Hallerud, Margaret, Heim, Eric, Hahnenberger, Maura, Sukumaran, Suja, 2020. Plastic rain in protected areas of the United States. Science 368 (6496), 1257–1260.

Cai, Huiwen, Xu, Elvis Genbo, Du, Fangni, Li, Ruilong, Liu, Jingfu, Shi, Huahong, 2021. Analysis of environmental nanoplastics: Progress and challenges. Chem. Eng. J. 410, 128208.

Carpenter, Edward J., Smith, Jr., K.L., 1972. Plastics on the sargasso sea surface. Science 175 (4027), 1240–1241.

Chang, Lin, Jiang, Shan, Luo, Jie, Zhang, Jianfa, Liu, Xiaohong, Lee, Chong-Yew, Zhang, Wei, 2022. Nanowell-enhanced Raman spectroscopy enables the visualization and quantification of nanoplastics in the environment. Environ. Sci.: Nano 9 (2), 542–553.

Dawson, Amanda L, Kawaguchi, So, King, Catherine K, Townsend, Kathy A, King, Robert, Huston, Wilhelmina M, Bengtson Nash, Susan M, 2018. Turning microplastics into nanoplastics through digestive fragmentation by Antarctic krill. Nature Commun. 9 (1), 1001.

Dimante-Deimantovica, Inta, Saarni, Saija, Barone, Marta, Buhhalko, Natalja, Stivrins, Normunds, Suhareva, Natalija, Tylmann, Wojciech, Vianello, Alvise, Vollertsen, Jes, 2024. Downward migrating microplastics in lake sediments are a tricky indicator for the onset of the Anthropocene. Sci. Adv. 10 (8), eadi8136.

Du, Fangni, Cai, Huiwen, Su, Lei, Wang, Wei, Zhang, Liwu, Sun, Chengjun, Yan, Beizhan, Shi, Huahong, 2024. The missing small microplastics: easily generated from weathered plastic pieces in labs but hardly detected in natural environments. Environ. Sci.: Adv..

Ehrlich, Hermann, Demadis, Konstantinos D, Pokrovsky, Oleg S, Koutsoukos, Petros G, 2010. Modern views on desilicification: biosilica and abiotic silica dissolution in natural and artificial environments. Chem. Rev. 110 (8), 4656–4689.

El Hadri, Hind, Gigault, Julien, Maxit, Benoit, Grassl, Bruno, Reynaud, Stéphanie, 2020. Nanoplastic from mechanically degraded primary and secondary microplastics for environmental assessments. NanoImpact 17, 100206.

Ferrari, Andrea C., 2007. Raman spectroscopy of graphene and graphite: Disorder, electron–phonon coupling, doping and nonadiabatic effects. Solid State Commun. 143 (1–2), 47–57.

Geyer, Roland, Jambeck, Jenna R., Law, Kara Lavender, 2017. Production, use, and fate of all plastics ever made. Sci. Adv. 3 (7), e1700782.

Gigault, Julien, Pedrono, Boris, Maxit, Benoît, Ter Halle, Alexandra, 2016. Marine plastic litter: the unanalyzed nano-fraction. Environ. Sci.: Nano 3 (2), 346–350.

Gillibert, Raymond, Balakrishnan, Gireeshkumar, Deshoules, Quentin, Tardivel, Morgan, Magazzù, Alessandro, Donato, Maria Grazia, Maragò, Onofrio M., Lamy de La Chapelle, Marc, Colas, Florent, Lagarde, Fabienne, Gucciardi, Pietro G., 2019. Raman tweezers for small microplastics and nanoplastics identification in seawater. Environ. Sci. Technol. 53 (15), 9003–9013, PMID: 31259538.

Gulizia, Alexandra M, Brodie, Eve, Daumuller, Renee, Bloom, Sarah B, Corbett, Tayla, Santana, Marina MF, Motti, Cherie A, Vamvounis, George, 2022. Evaluating the effect of chemical digestion treatments on polystyrene microplastics: Recommended updates to chemical digestion protocols. Macromol. Chem. Phys. 223 (13), 2100485.

Hernandez, Laura M, Grant, Joel, Fard, Parvin Shakeri, Farner, Jeffrey M, Tufenkji, Nathalie, 2023. Analysis of ultraviolet and thermal degradations of four common microplastics and evidence of nanoparticle release. J. Hazard. Mater. Lett. 4, 100078.

Hernandez, Laura M, Xu, Elvis Genbo, Larsson, Hans CE, Tahara, Rui, Maisuria, Vimal B, Tufenkji, Nathalie, 2019. Plastic teabags release billions of microparticles and nanoparticles into tea. Environ. Sci. Technol. 53 (21), 12300–12310.

Hu, Rui, Zhang, Kaining, Wang, Wei, Wei, Long, Lai, Yongchao, 2022a. Quantitative and sensitive analysis of polystyrene nanoplastics down to 50 nm by surface-enhanced Raman spectroscopy in water. J. Hazard. Mater. 429, 128388.

Hu, Rui, Zhang, Kaining, Wang, Wei, Wei, Long, Lai, Yongchao, 2022b. Quantitative and sensitive analysis of polystyrene nanoplastics down to 50 nm by surface-enhanced Raman spectroscopy in water. J. Hazard. Mater. 429, 128388.

Ivleva, Natalia P., Wiesheu, Alexandra C., Niessner, Reinhard, 2017. Microplastic in aquatic ecosystems. Angew. Chem. Int. Ed. 56 (7), 1720–1739.

Leslie, Heather A, Van Velzen, Martin Jm, Brandsma, Sicco H, Vethaak, A Dick, Garcia-Vallejo, Juan J, Lamoree, Marja H, 2022. Discovery and quantification of plastic particle pollution in human blood. Environ. Int. 163, 107199.

Li, Dunzhu, Shi, Yunhong, Yang, Luming, Xiao, Liwen, Kehoe, Daniel K, Gun'ko, Yurii K, Boland, John J, Wang, Jing Jing, 2020. Microplastic release from the degradation of polypropylene feeding bottles during infant formula preparation. Nature Food 1 (11), 746–754.

Lim, XiaoZhi, et al., 2021. Microplastics are everywhere—but are they harmful. Nature 593 (7857), 22–25.

Löder, Martin G.J., Imhof, Hannes K., Ladehoff, Maike, Löschel, Lena A., Lorenz, Claudia, Mintenig, Svenja, Piehl, Sarah, Primpke, Sebastian, Schrank, Isabella, Laforsch, Christian, Gerdts, Gunnar, 2017. Enzymatic purification of microplastics in environmental samples. Environ. Sci. Technol. 51 (24), 14283–14292, PMID: 29110472.

Lv, Lulu, He, Lei, Jiang, Shiqi, Chen, Jinjun, Zhou, Chunxia, Qu, Junhao, Lu, Yuqin, Hong, Pengzhi, Sun, Shengli, Li, Chengyong, 2020. In situ surface-enhanced Raman spectroscopy for detecting microplastics and nanoplastics in aquatic environments. Sci. Total Environ. 728, 138449.

Mandemaker, Laurens D.B., Meirer, Florian, 2023. Spectro-microscopic techniques for studying nanoplastics in the environment and in organisms. Angew. Chem. Int. Ed. 62 (2), e202210494.

Materić, Dušan, Holzinger, Rupert, Niemann, Helge, 2022a. Nanoplastics and ultrafine microplastic in the Dutch Wadden Sea – the hidden plastics debris? Sci. Total Environ. 846, 157371.

Materić, Dušan, Kasper-Giebl, Anne, Kau, Daniela, Anten, Marnick, Greilinger, Marion, Ludewig, Elke, van Sebille, Erik, Röckmann, Thomas, Holzinger, Rupert, 2020. Micro-and nanoplastics in alpine snow: a new method for chemical identification and (semi) quantification in the nanogram range. Environ. Sci. Technol. 54 (4), 2353–2359.

Materić, Dušan, Peacock, Mike, Dean, Joshua, Futter, Martyn, Maximov, Trofim, Moldan, Filip, Röckmann, Thomas, Holzinger, Rupert, 2022b. Presence of nanoplastics in rural and remote surface waters. Environ. Res. Lett. 17 (5), 054036.

Mattsson, Karin, Hagberg, Mats, Hassellöv, Martin, 2024. Platinum vaporization-deposition coated polycarbonate membranes for comprehensive, multimodal, and correlative microscopic analysis of micro-and nanoplastics and other environmental particles. Talanta 269, 125435.

Minelli, Caterina, Sikora, Aneta, Garcia-Diez, Raul, Sparnacci, Katia, Gollwitzer, Christian, Krumrey, Michael, Shard, Alex G, 2018. Measuring the size and density of nanoparticles by centrifugal sedimentation and flotation. Anal. Methods 10 (15), 1725–1732.

Moon, Seunghyun, Martin, Leisha MA, Kim, Seongmin, Zhang, Qiushi, Zhang, Renzheng, Xu, Wei, Luo, Tengfei, 2024. Direct observation and identification of nanoplastics in ocean water. Sci. Adv. 10 (4), eadh1675.

Oßmann, Barbara E, Sarau, George, Schmitt, Sebastian W, Holtmannspötter, Heinrich, Christiansen, Silke H, Dicke, Wilhelm, 2017. Development of an optimal filter substrate for the identification of small microplastic particles in food by micro-Raman spectroscopy. Anal. Bioanal. Chem. 409, 4099–4109.

Pfeiffer, Felix, Fischer, Elke Kerstin, 2020. Various digestion protocols within microplastic sample processing—evaluating the resistance of different synthetic polymers and the efficiency of biogenic organic matter destruction. Front. Environ. Sci. 8, 572424.

Ragusa, Antonio, Svelato, Alessandro, Santacroce, Criselda, Catalano, Piera, Notarstefano, Valentina, Carnevali, Oliana, Papa, Fabrizio, Rongioletti, Mauro Ciro Antonio, Baiocco, Federico, Draghi, Simonetta, et al., 2021. Plasticenta: First evidence of microplastics in human placenta. Environ. Int. 146, 106274.

Saarni, Saija, Hartikainen, Samuel, Meronen, Senja, Uurasjärvi, Emilia, Kalliokoski, Maarit, Koistinen, Arto, 2021. Sediment trapping–an attempt to monitor temporal variation of microplastic flux rates in aquatic systems. Environ. Pollut. 274, 116568.

Schmidt, Ruth, Nachtnebel, Manfred, Dienstleder, Martina, Mertschnigg, Sabrina, Schroettner, Hartmuth, Zankel, Armin, Poteser, Michael, Hutter, Hans-Peter, Eppel, Wolfgang, Fitzek, Harald, 2021. Correlative SEM-Raman microscopy to reveal nanoplastics in complex environments. Micron 144, 103034.

Schwaferts, Christian, Sogne, Vanessa, Welz, Roland, Meier, Florian, Klein, Thorsten, Niessner, Reinhard, Elsner, Martin, Ivleva, Natalia P., 2020. Nanoplastic analysis by online coupling of Raman microscopy and field-flow fractionation enabled by optical tweezers. Anal. Chem. 92 (8), 5813–5820, PMID: 32073259.

Sharma, Bhavya, Frontiera, Renee R, Henry, Anne-Isabelle, Ringe, Emilie, Van Duyne, Richard P, 2012. SERS: Materials, applications, and the future. Mater. Today 15 (1–2), 16–25.

Sobhani, Zahra, Zhang, Xian, Gibson, Christopher, Naidu, Ravi, Megharaj, Mallavarapu, Fang, Cheng, 2020. Identification and visualisation of microplastics/nanoplastics by Raman imaging (i): Down to 100 nm. Water Res. 174, 115658.

Stiles, Paul L., Dieringer, Jon A., Shah, Nilam C., Van Duyne, Richard P., 2008. Surface-enhanced Raman spectroscopy. Annu. Rev. Anal. Chem. 1 (1), 601–626, PMID: 20636091.

Venrick, EL, Backman, TW, Bartram, WC, Platt, CJ, Thornhill, MS, Yates, RE, 1973. Man-made objects on the surface of the central north Pacific ocean. Nature 241 (5387), 271–271.

Wahl, Aurélie, Le Juge, Corentin, Davranche, Mélanie, El Hadri, Hind, Grassl, Bruno, Reynaud, Stephanie, Gigault, Julien, 2021. Nanoplastic occurrence in a soil amended with plastic debris. Chemosphere 262, 127784.

Way, Chloe, Hudson, Malcolm D, Williams, Ian D, Langley, G John, 2022. Evidence of underestimation in microplastic research: a meta-analysis of recovery rate studies. Sci. Total Environ. 805, 150227.

Winkler, Anna, Fumagalli, Francesco, Cella, Claudia, Gilliland, Douglas, Tremolada, Paolo, Valsesia, Andrea, 2022. Detection and formation mechanisms of secondary nanoplastic released from drinking water bottles. Water Res. 222, 118848.

Xu, Guanjun, Cheng, Hanyun, Jones, Robin, Feng, Yiqing, Gong, Kedong, Li, Kejian, Fang, Xiaozhong, Tahir, Muhammad Ali, Valev, Ventsislav Kolev, Zhang, Liwu, 2020. Surface-enhanced Raman spectroscopy facilitates the detection of microplastics <1 um in the environment. Environ. Sci. Technol. 54 (24), 15594–15603, PMID: 33095569.

Yang, Tong, Luo, Jialuo, Nowack, Bernd, 2021. Characterization of nanoplastics, fibrils, and microplastics released during washing and abrasion of polyester textiles. Environ. Sci. Technol. 55 (23), 15873–15881, PMID: 34784483.

Yang, Qing, Zhang, Shaoying, Su, Jie, Li, Shu, Lv, Xiaochen, Chen, Jing, Lai, Yongchao, Zhan, Jinhua, 2022. Identification of trace polystyrene nanoplastics down to 50 nm by the hyphenated method of filtration and surface-enhanced Raman spectroscopy based on silver nanowire membranes. Environ. Sci. Technol. 56 (15), 10818–10828.

Yoo, Hanjin, Lee, Hayeong, Park, Changmin, Shin, Dongha, Ro, Chul-Un, 2022. Novel single-particle analytical technique for submicron atmospheric aerosols: Combined use of dark-field scattering and surface-enhanced Raman spectroscopy. Anal. Chem. 94 (38), 13028–13035, PMID: 36107822.

Zhang, Wen, Dong, Zhiqiang, Zhu, Ling, Hou, Yuanzhang, Qiu, Yuping, 2020. Direct observation of the release of nanoplastics from commercially recycled plastics with correlative Raman imaging and scanning electron microscopy. ACS Nano 14 (7), 7920–7926, PMID: 32441911.

Zou, Taoyu, Chang, Jiawei, Chen, Qiuyuan, Nie, Zhifeng, Duan, Liangfei, Guo, Tingting, Song, Yumin, Wu, Wei, Wang, Hai, 2020. Novel strategy for organic cocrystals of n-type and p-type organic semiconductors with advanced optoelectronic properties. ACS Omega 5 (21), 12067–12072.